Unoccupied electronic structure of Al(111)

S. Yang,* R. A. Bartynski, and David Vanderbilt

*Department of Physics and Astronomy and the Laboratory for Surface Modification, Rutgers University,
Piscataway, New Jersey 08855-0849*

The unoccupied electronic states of the Al(111) surface have been studied using k-resolved inverse-photoemission spectroscopy (KRIPES). In addition, a first-principles calculation of the bulk Al electronic structure has been performed to facilitate interpretation of the experimental data. The KRIPES spectra obtained along the $[\bar{1}10]$, $[11\bar{2}]$, and $[\bar{1}\,\bar{1}2]$ azimuths of the surface Brillouin zone are characterized by well-defined features within 5 eV of the Fermi level, and broad, weak features at higher energies. In general, surface states and resonances appeared as strong spectral features while bulk transitions were weak for this surface. First-principles electronic-structure calculations were necessary to obtain a qualitative account of the bulk features, and semiquantitative agreement was obtained when excitation effects were considered. Dispersion of an unoccupied surface resonance along the $[11\bar{2}]$ azimuth is consistent both with an occupied surface resonance found by an earlier photoemission study and with the predictions of surface electronic-structure calculations in the literature. A strong feature observed in the $[\bar{1}12]$ direction is identified as an odd surface state occurring in a symmetry gap and may account for earlier electron-energy-loss data.

I. INTRODUCTION

Aluminum is often considered to be a text book example of a nearly-free-electron (NFE) metal. This model system can also serve as a stringent test for both theoretical and experimental techniques for determining the electronic structure of solids. Early studies of aluminum's electronic structure focused on determining the Fermi surface[1] and understanding the low-energy optical excitations[2,3] of the bulk. In general, these measurements are well described by the nearly-fee-electron model. Detailed experimental investigations of aluminum's bulk and surface electronic structure away from the Fermi level became possible with the advent of angle-resolved photoemission spectroscopy.[4-6] In measurements of the occupied bulk band structure,[4] the valence-band width was found to be significantly narrower, and the band gaps were wider, than predicted by the NFE simple theory. First-principles calculations provided a closer correspondence between theory and experiment, but consideration of the nonlocal part of the electron self-energy was necessary to obtain quantitative agreement. Similar trends have now been observed for other "simple" metals[7-10] and have been attributed to electron excitation effects and deficiencies in the local-density approximation. These materials may be free-electron-like, but they are certainly not simple.

Angle-resolved photoemission has also been used to probe the unoccupied electronic structure of aluminum well above the Fermi level (E_F).[4] Along the Δ line of the bulk Brillouin zone, the experimentally determined band structure at energies greater than ~ 50 eV above E_F is well described by a free-electron band with unity effective mass. Between 30 and 35 eV, a large band gap occurs while for energies below 25 eV no direct transitions are

observed. Although the band structure of Al is quite complicated at these energies,[11] the photoemission data only sampled the portion of the bands with substantial free-electron-like components propagating normal to the surface.[4]

In contrast, little is known about the unoccupied electronic structure of Al near the Fermi level. This is an extremely important energy range since these states directly participate in the low-energy excitations of the system. Although inverse photoemission[12-14] (IPE) is an ideal probe of these unoccupied electronic states since it can access states between the Fermi level and the vacuum level (E_{vac}), no thorough IPE study of Al has been reported. As part of a larger study of alkali metals, Heskett et al.[15] reported a normal-incidence spectrum from the clean Al(111) surface that exhibited a single feature pinned to the vacuum level and attributed this peak to an image-potential resonance. A more recent study[16] conducted with variable photon energy reported resonances in the inverse-photoemission cross section associated with the plasmon energy and interpreted this phenomenon as the inverse-photoemission analog of the surface photoeffect.[17-19]

In this paper, we present a combined experimental and theoretical study of the unoccupied surface and bulk electronic states of Al(111). Isochromat inverse-photoemission data were obtained along the $[\bar{1}10]$, $[11\bar{2}]$, and $[\bar{1}\,\bar{1}2]$ directions of the surface Brillouin zone (SBZ). To facilitate the interpretation of the experimental data, we have performed both NFE model and first-principles electronic-structure calculations for bulk Al. The results are discussed in the light of the limitation of the NFE model and the deficiencies of the independent-electron approximation. Along with bulk-related spectral features, we have identified several IPE features as surface states or resonances.

The image-potential resonance of Al(111), observed by Heskett et al.,[15] is a very interesting feature of this surface.[15,20−23] Image-potential states have been observed on many metal surfaces with inverse photoemission. The binding energy and dispersion of these states have been well described by the simple phase-analysis model[24] of electron scattering from the image potential and the crystal potential. The Al(111) surface differs from the equivalent surfaces of the fcc transition and noble metals in that it has no projected band gaps in the energy range of $E_F - E_{vac}$ near the center of the SBZ. Observation[15,25] of an image-potential resonance has excited considerable theoretical interest.[26−29] Most models associate the spectral feature with an enhanced surface density of states[26−28] owing to scattering either from an abrupt truncation of the image potential[28] or from the pseudopotential of the Al lattice.[26] An alternative and controversial explanation[29] attributes the observed spectral feature to oscillatory structure occurring in the calculated IPE transition matrix element due to an interference between the initial and final states. We believe that scattering from the Al pseudopotential is responsible for this feature. These ideas have been addressed in a previous publication,[20] and we will not discuss them further here.

The remainder of this paper is organized as follows. Section II describes the experimental apparatus and procedures as well as theoretical approaches used in our calculations. In Sec. III we present and interpret the experimental and theoretical results. Finally, Sec. IV summarizes this study.

II. EXPERIMENTAL AND COMPUTATIONAL DETAILS

The angle-resolved inverse-photoemission experiments were performed in the isochromat mode. Our experimental setup has been described in detail elsewhere.[30] Briefly, a well-collimated beam of low-energy electrons $(4 < E < 18$ eV) is directed onto the sample. Photons generated via radiative decay of these electrons inside the metal are detected by an I_2-filled Geiger-Müller tube with a SrF_2 window providing an operating energy of $\hbar\omega = 9.5 \pm 0.2$ eV. The spectrometer was housed in an ultrahigh-vacuum (UHV) chamber with a base pressure of 8×10^{-11} torr and equipped with Auger electron spectroscopy (AES) and low-energy electron diffraction (LEED) for surface characterization.

A single-crystal Al sample was oriented with its (111) axis within 1° of the surface normal by Laue x-ray diffraction, and then mechanically polished and chemically etched prior to insertion into the UHV chamber. Once in the spectrometer, many cycles of sputtering with 1-keV Ne^+ ions followed by annealing to 410 °C were needed to remove the native oxide layers and to deplete impurities (primarily carbon) in the near-surface region. Following this initial treatment, a clean and well-ordered Al(111) surface was obtained, characterized by a sharp (1×1) LEED pattern and the absence of discernible AES features associated with C,O, or other contaminants. No evidence of surface contamination by the residual gas was observed for periods of 8 h. Typically, the surface was recleaned every 5 h by a short (5-min) sputter with 500-

eV Ne^+ followed by a 20-min anneal at 410 °C.

The theoretical valence-band electronic structure of aluminum was calculated using both an empirical pseudopotential obtained from the literature and a first-principles, self-consistent pseudopotential. In the former, two Fourier coefficients,[31] V_{111} ($=0.0179$ Ry) and V_{200} ($=0.0562$ Ry), were included. The latter was generated from the Hamann-Schlüter-Chiang scheme[32] and optimally smoothed.[33] This calculation employed plane waves with kinetic energies up to 16 Ry.

III. RESULTS AND DISCUSSION

Aluminum has a fcc crystal structure. Figure 1 illustrates the real and reciprocal space unit cells of the fcc (111) surface. The real space drawing indicates the stacking sequence of the fcc structure. Note that the $[11\bar{2}]$ and $[\bar{1}\,\bar{1}2]$ directions, which are degenerate in the two-dimensional (2D) unit net, are inequivalent when the bulk structure is considered. In this paper, we will restrict our discussion to the three high-symmetry directions, $[\bar{1}10]$, $[11\bar{2}]$, and $[\bar{1}\,\bar{1}2]$, as indicated in the figure.

A. $\bar{\Gamma}$ - $\bar{K}$, the $[\bar{1}10]$ direction

In Fig. 2(a), we present k-resolved inverse-photoemission spectra (KRIPES) obtained for a series of different incident electron angles θ along the $[\bar{1}10]$ azimuth of the surface Brillouin zone. In these and all subsequent spectra, the solid lines are digital smoothing to the raw data (represented by dots). Near normal incidence, the spectrum exhibits a single peak ~ 4 eV above the Fermi level. This feature, which we label IR, corresponds to the image-potential resonance at the center of the SBZ, previously observed by Heskett et al.[15] For $\theta > 10°$, several broad, weak features are observed at energies greater than ~ 5 eV. It is not clear whether these features consist of a single broad peak or are composed of several weak overlapping features. The most prominent peaks and shoulders in the spectra are indicated by the
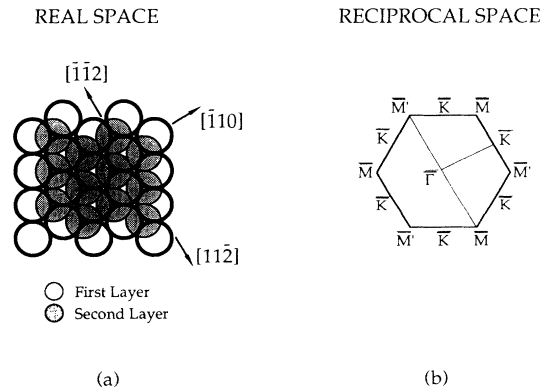

FIG. 1. Geometry of the fcc (111) surface in (a) real space and (b) reciprocal space. Note that the inequivalence of the $[11\bar{2}]$ and $[\bar{1}\,\bar{1}2]$ directions is illustrated by the presence of the second layer in panel (a).
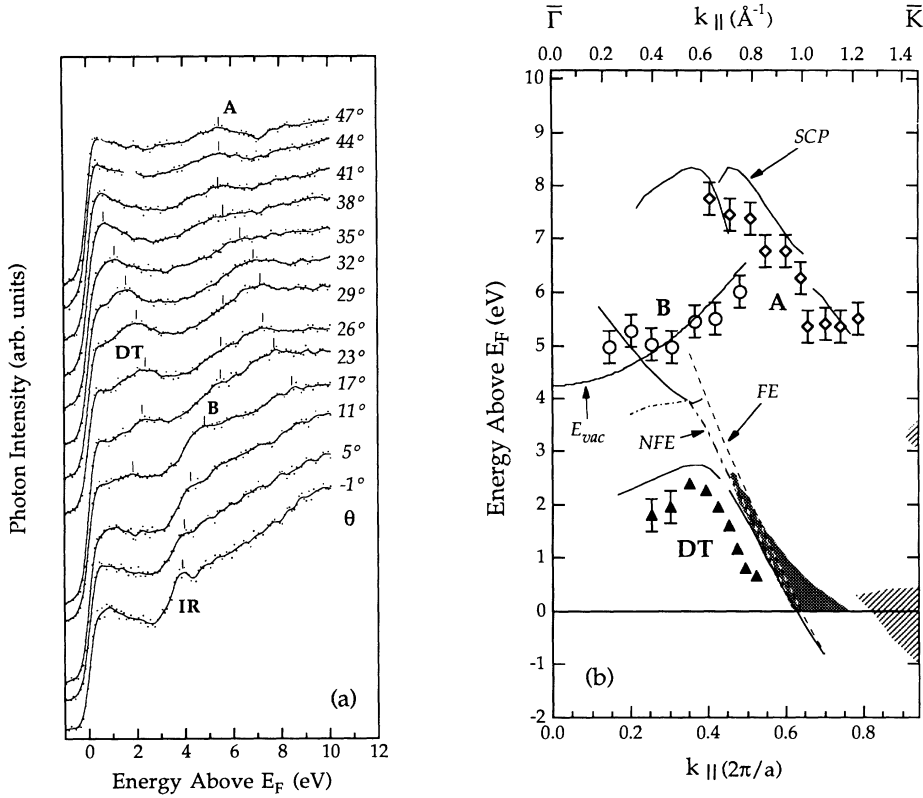
FIG. 2. (a) KRIPE isochromat spectra from Al(111) as a function of incident electron angle θ along the $[\bar{1}10]$ ($\bar{\Gamma} \rightarrow \bar{K}$) azimuth of the Al(111) SBZ with $\hbar\omega = 9.5$ eV. (b) Dispersion plot of experimentally observed features (labeled as DT, A, and B) and theoretically calculated direct bulk transitions along the ($\bar{\Gamma} \rightarrow \bar{K}$) azimuth. Results assuming free-electron (FE), nearly-free-electron (NFE), and the self-consistent l-dependent pseudopotential (SCP) bands are given by the dashed, dashed-and-dotted, and solid curves, respectively. Hatched areas indicate the projected bulk band gaps and shaded area shows a predicted surface resonance (Ref. 37).

tick marks labeled A and B. At energies below 4 eV, a single well-defined peak appears near $\theta = 15°$. This peak disperses to higher energy with increasing angle, reaching a maximum value of 2.3 eV at $\theta = 26°$. For larger incident angles, the peak moves towards lower energies, eventually crossing the Fermi level near $\theta = 38°$.

To facilitate comparison with the theoretically predicted electronic structure, the energies of features A, B, and DT are plotted in Fig. 2(b) as a function of $k_\parallel$, the component of the electron momentum parallel to the surface. The magnitude of $k_\parallel$ is given by $k_\parallel = \sqrt{2mE_k/\hbar^2}\sin\theta$, where $E_k = E_{\text{fin}} + \hbar\omega - \phi$ is the kinetic energy of the incident electron, E_{fin} the peak energy in our spectra (referenced to E_F), and ϕ the sample work function. Along this azimuth of the SBZ, the projected bulk bands encompass the entire range of this figure except for two small gaps [hatched areas in Fig. 2(b)] at the zone boundary. We also plot in Fig. 2(b) the final-state dispersion curves for the direct transitions (at $\hbar\omega = 9.5$ eV) predicted by the self-consistent l-dependent pseudopotential (SCP) calculations. Only those direct transitions with final-state energies in the vicinity of the IPE spectral features and initial-state wave functions composed primarily of the same plane waves as the incident electrons are included in the figure. Owing to the numerous transitions predicted at higher energies and the broad nature of spectral features observed, precise determination of the origin of these high-energy peaks is difficult; nevertheless, they are most likely related to the bulk band structure. The motion of feature B appears to follow the dispersion of

the vacuum level and may be related to the surface continuum.[21] Focusing our discussion on the well-defined feature DT, Fig. 2(b) shows that this feature overlaps the projected bulk band structure, indicating that it is either a bulk direct transition or a surface resonance. As we are limited experimentally to a photon energy of 9.5 eV, we cannot vary $k_\perp$ to distinguish between these possibilities. Furthermore, since the photon energy is smaller than the bulk plasma energy of Al (~ 15 eV), the weak coupling of the bulk electron gas to the photon field[16] implies that the inverse-photoemission signal originates primarily from the surface region. Consistent with these ideas, we find that surface contamination by the residual gas, or by intentional adsorption of oxygen, quenches all spectral features with approximately the same efficiency, rendering the so-called "crud test" inconclusive. Therefore, to aid in identifying this feature we turn to previous photoemission experiments and theoretical calculations.

Along the $\bar{\Gamma}$-$\bar{K}$ azimuth, a surface resonance was predicted by Wang et al.[34] This surface resonance, originating from an occupied surface state located at ~ 0.58 eV below the Fermi level at $\bar{K}$, disperses upward as $k_\parallel$ moves away from $\bar{K}$. A similar state has also been found in other self-consistent calculations.[35,36] A very recent first-principles slab calculation[37] found that this surface state becomes a "broad" surface resonance when it enters the projected bulk bands and disperses above the Fermi level. The predicted location of this resonance, shown by the shaded region of Fig. 2(b), is not consistent with the region of $k_\parallel$ in which DT is observed. The existence of an

occupied surface state in this gap has been confirmed by angle-resolved photoemission experiments.[5] However, it was found[5] that this feature disperses very rapidly towards E_F and only exists in a small range of $\Delta k_{\parallel} = 0.3$ Å^{-1} about $\bar{K}$. It is doubtful that this feature and DT are related, since DT crosses the Fermi level in a very different part of the SBZ as shown in Fig. 2(b). Owing to limitations in the experimental geometry, we were unable to access the values of $k_{\parallel}$ where this broad resonance is predicted.

The remaining possibility is that DT is a bulk direct transition. It is instructive to consider predicted direct transitions at $\hbar\omega = 9.5$ eV based on several approximations for the bulk band structure to assess how well ground-state band-structure calculations can account for the experimentally observed unoccupied states of a simple metal. This exercise illustrates that even for "simple" metals, first-principles calculations are needed for a full understanding of their electronic properties. The dashed curve (labeled FE) in Fig. 2(b) shows the dispersion of a direct transition between two Al bands that were calculated within the free-electron model. Although the trend of the experimental data is well reproduced near $k_{\parallel} = 0.75$ Å^{-1}, the agreement diminishes as $k_{\parallel}$ decreases and finally breaks down, even qualitatively, for $k_{\parallel} < 0.6$ Å^{-1}. Comparing our data to transitions based on the empirical pseudopotential calculation (dashed-and-dotted curve labeled NFE) yields little improvement over the free-electron results. This is somewhat surprising since the same pseudopotential calculations accurately describe low-energy optical excitations.[2,3] We attribute the lack of agreement in the IPE case to the fact that the initial states are between 10 and 12 eV above the Fermi level, an energy range where these model calculations are not expected to be accurate. It is interesting to note that, though still 1.5 eV above the experimental dispersion for $0.3 < k_{\parallel} < 0.6$ Å^{-1}, a branch in the NFE calculation has moved significantly closer to the experimental data than its FE counterpart (not shown).

The solid line in Fig. 2(b) gives the predicted direct transitions from the self-consistent pseudopotential calculation. In contrast to the two previous cases, the shape of the experimental dispersion is well reproduced and the energy separation is relatively small throughout the entire range of $k_{\parallel}$ over which DT is observed. This is in part due to the improved accuracy with which states having significant d character are describe using the l-dependent pseudopotential. Based on the FE and NFE models alone, it would have been extremely difficult to identify the bands in the $0.3 < k_{\parallel} < 0.6$ Å^{-1} region that were responsible for the experimental data.

Despite the significantly better agreement obtained with the self-consistent calculation, the predicted direct transitions still consistently lie ~ 0.5 eV above the experimental points. There are several possible reasons for this result. First it is possible that the initial states are not well described by the calculation. Based on comparison with other calculations[11] of the Al electronic structure, and on similar calculations performed for other materials, we feel that this explanation is unlikely. On the other hand, a similar disagreement between photoemission

data[4] and first-principles calculations[11] of the occupied states led to the conclusion[4] that excitation effects were responsible. Early theoretical work[38] addressing the electron self-energy in the uniform electron gas found that these corrections shifted the one-electron results towards the Fermi level. Recent estimates[39] of the electron self-energy in Al indicate that the difference in this correction is about 0.5 eV greater at 12 eV above E_F than it is at 2 eV. These corrections would bring the predicted direct transitions into excellent agreement with the experimental measurements. Similar arguments have been used to account for the reduction in bandwidth observed in photoemission experiments from several other simple metals.[7–10,40]

B. $\bar{\Gamma}$-$\bar{M}$, the [11$\bar{2}$] direction

Spectra obtained at different incident electron angles along the [11$\bar{2}$] azimuth of the Al(111) surface are presented in Fig. 3(a). Similar to the [$\bar{1}$10] direction, the image-potential resonance IR is observed near normal incidence and several broad features (labeled as A' and B') occur at high energies in spectra taken at larger incident angles. We will focus on the distinct feature labeled SR observed at low energies. This feature first appears near $\theta = 20°$, getting narrower and more intense as it disperses to lower energy, finally crossing the Fermi level near $\theta = 45°$.

The dispersions with $k_{\parallel}$ of the features identified in Fig. 3(a) are plotted in Fig. 3(b). As was seen along [$\bar{1}$10], the high-energy features are roughly consistent with predicted direct transitions. In contrast to the case of DT, however, there are no direct transitions near the low-energy feature SR with initial states that couple favorably to the wave function of the incident electron. On the other hand, Fig. 3(b) shows that, as SR disperses towards the Fermi level, it leads into an occupied surface resonance observed in an early angle-resolved photoemission experiment by Hansson and Flodström.[6] This surface resonance was identified in the self-consistent slab calculations of Wang et al.[34] and the theoretical dispersion matches Hansson and Flodström's photoemission data almost perfectly. Unfortunately, this calculation did not report on the states above the Fermi level. The recent calculation of Heinrichsmeier, Fleszar, and Eguiluz[37] predicts the same surface resonance and determines its dispersion into the unoccupied states. The shaded region in Fig. 3(b) shows the results of this calculation and we find that they are in excellent agreement with our experimental measurements. A sharp Σ_1 surface resonance was also predicted[37] to occur near the SBZ boundary. However, our experiments do not extend to a sufficiently large angle to examine this region of energy-momentum space.

The origin of the surface resonance along $\bar{\Gamma}$-$\bar{M}$ can be understood by considering the bulk bands at a fixed $k_{\parallel}$ as suggested by Wang et al.[34] The results of our self-consistent pseudopotential calculation for $k_{\parallel} = 0.782$ Å^{-1} in the energy region of interest are shown in Fig. 4(a). For the kinematically favored direct transitions, only bands on the positive $k_{\perp}$ side are important in this discussion. These bands are shown in bold in Fig. 4(a). Note
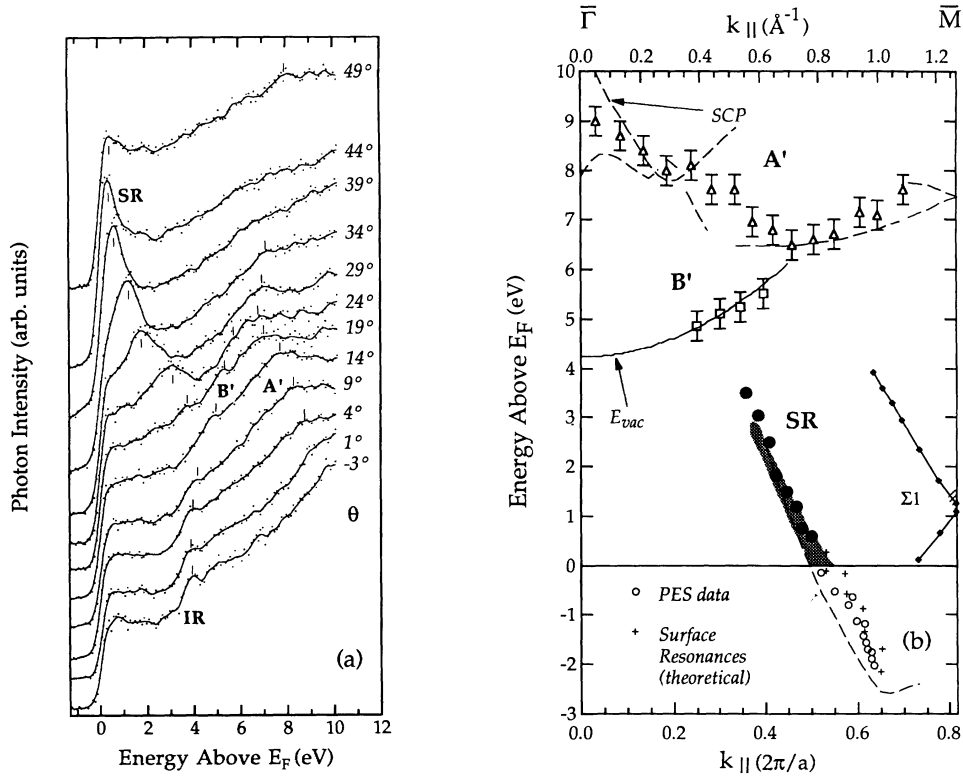
FIG. 3. (a) KRIPE iso-chromat spectra from Al(111) as a function of incident electron angle θ along the $[11\bar{2}]$ $(\bar{\Gamma} \rightarrow \bar{M})$ azimuth of the Al(111) SBZ with $\hbar\omega = 9.5$ eV. (b) Dispersion plot of experimentally observed features (labeled as SR, A', and B') and theoretically calculated direct bulk transitions (dashed lines) along the $[11\bar{2}]$ $(\bar{\Gamma} \rightarrow \bar{M})$ azimuth. Relevant calculated direct transition curves from the SCP bands are shown. Photo-emission data (open circles) (Ref. 6) and the calculated (Ref. 32) dispersion of a surface resonance (crosses) are included for comparison. The hatched area indicates the projected bulk band gap and the shaded area shows the predicted (Ref. 37) disper-sion of the surface resonance above E_F.

that a gap exists between the second and third bands at $k_{\perp} \approx 1.1$ Å^{-1}. However, bulk states from the second band cross the gap at $k_{\perp} \approx 0.6$ Å^{-1} (and again at $k_{\perp} \sim -0.9$ Å^{-1}) and therefore a band gap will not appear when the bulk bands are projected into the surface Brillouin zone. If, on the other hand, a state were only slightly split off the third band near $k_{\perp} \approx 1.1$ Å^{-1}, its wave function would be composed predominantly of Bloch states near that $k_{\perp}$.[41] Therefore, it may not couple strongly to the second band at a very different $k_{\perp}$. We refer to this sort of feature in the band structure as a quasi-band-gap. In Fig. 4(b), we track the energy of the quasigap near E_F as a function of $k_{\parallel}$ and find that, similar to the photoemission results,[6] its motion is almost identical to that of SR and the surface resonance predicted by Heinrichsmeier, Fleszar, and Eguiluz.[37]

It is interesting to note that both SR and the occupied surface resonance[6] exhibit a strong enhancement of spec-tral intensity as they move towards the Fermi level. This is consistent with the band-structure calculation, since
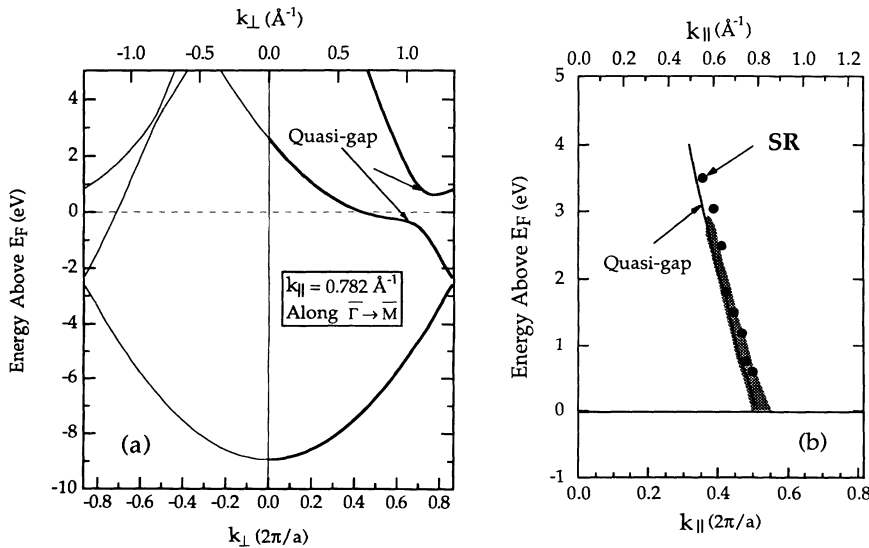

FIG. 4. (a) Self-consistent pseudopotential calculation for Al(111) bulk electron energy bands as a function of $k_{\perp}$ at $k_{\parallel} = 0.782$ Å^{-1} along the $[11\bar{2}](\bar{\Gamma} \rightarrow \bar{M})$ azimuth of the SBZ. Indicated is the quasi-band-gap. (b) Comparison of the $E(k_{\parallel})$ dispersions, along the $[11\bar{2}]$ $(\bar{\Gamma} \rightarrow \bar{M})$ azimuth of the Al(111) SBZ, of the quasi-band-gap from panel (a) and the KRIPE spectral feature SR.

the nature of the quasigap approaches that of a projected band gap as the Fermi level crossing is approached from above and below. In addition, owing to the surface photoeffect, we expect that states whose wave functions are enhanced at the surface will contribute more strongly to the inverse photoemission spectrum.

C. $\overline{\Gamma}$-$\overline{M}'$, the $[\bar{1}\bar{1}2]$ direction

Inverse-photoemission spectra obtained along the $[\bar{1}\bar{1}2]$ direction are presented in Fig. 5(a). For $\theta < 30°$, the spectra are qualitatively similar to those obtained for the other two high-symmetry directions in that the feature IR dominates near normal incidence and broad features at high energies are seen away from the center of the SBZ. In contrast to the other directions, however, two well-defined features, labeled $T1$ and $T2$ in Fig. 5(a), are observed dispersing towards the Fermi level with increasing angle. Ultimately $T1$ and $T2$ reach minimum energies of 2.4 and 4.0 eV, respectively, at angles corresponding to the $\overline{M}'$ point on the SBZ boundary. We refer to $T1$ and $T2$ as the "twin peaks" owing to the similarity in their dispersions.

To establish the origin of these features, we consider the direct transitions predicted by our self-consistent pseudopotential calculation given by the dashed lines in Fig. 5(b). As observed earlier, a number of possible direct transitions may account for the high-energy features. At lower energies, the surface resonance along $\overline{\Gamma}$-$\overline{M}$ from the slab calculations[37] is also shown as the shaded area. No experimental features corresponding to this resonance are found, most likely owing to the fact that the $k_\perp$ components of the plane waves that compose the bulk states

neighboring this surface resonance have the opposite signs in the $\overline{\Gamma}$-$\overline{M}'$ and $\overline{\Gamma}$-$\overline{M}$ directions. Feature $T1$ is consistent with a direct transition, given by the dashed curve, whose initial state couples favorably with the incident electron [a large component corresponding to the free-electron band with $g = (-1, -1, -1)$]. A sharp Σ_1 surface resonance is also predicted by the slab calculation[37] in the region near $T1$; however its dispersion is not consistent with that found experimentally. For $T2$ there are no predicted direct transitions within any model or of any symmetry, nor any surface resonances, that can be associated with this feature.

The comparison of $T1$ with the bulk electronic structure makes it a strong candidate for a direct transition. There are at least two pieces of evidence which support this interpretation. First, the spectral intensity of $T1$ is much weaker than that of $T2$. This is consistent with the weak (strong) intensity observed for bulk (surface) features along the other high-symmetry directions and is attributed to the photon energy used in this experiment. Second, although the predicted direct transition does not exactly coincide with $T1$, accounting for excitation effects,[39] as was done in Sec. III A, will raise the predicted transition in this case and improves agreement with our observations.

The origin of $T2$ is less obvious. Figure 6(a) is a plot of the bulk bands as a function of $k_\perp$ at the point $k_\parallel = 1.043$ Å^{-1} along the $[\bar{1}\bar{1}2]$ direction. Two quasi-band-gaps, indicated in the figure, occur in the region of $T1$ and $T2$. The energy of these gaps as a function of parallel momentum, along with the experimental dispersions of $T1$ and $T2$ is shown in Fig. 6(b). The lower quasigap is associated with the sharp surface resonance found in the calcula-
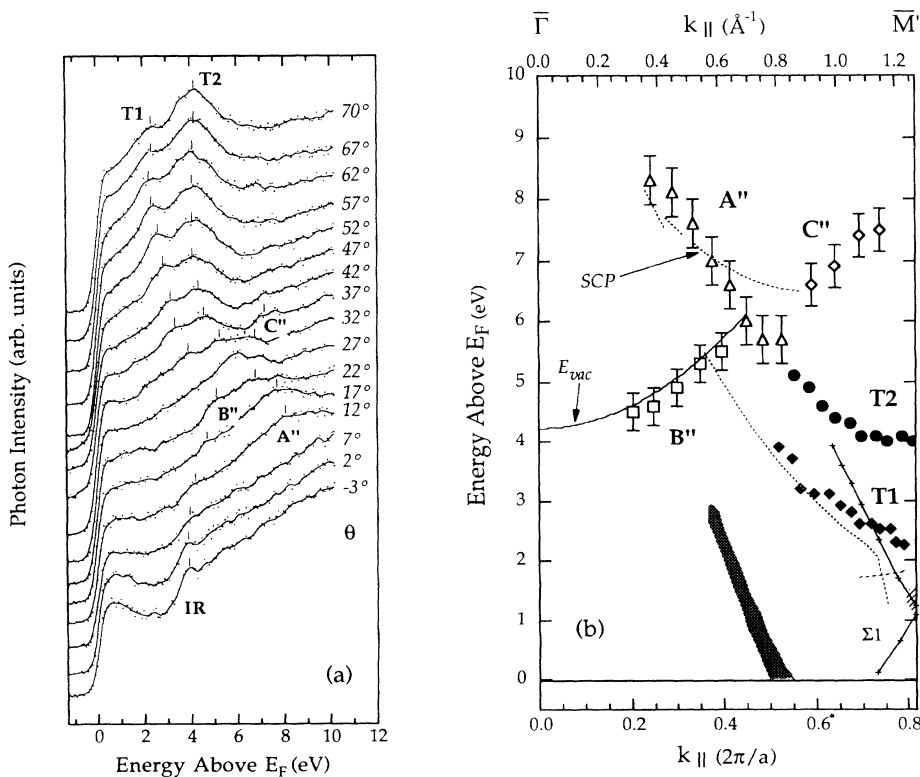

FIG. 5. (a) KRIPE isochromat spectra from Al(111) as a function of incident electron angle θ along $[\bar{1}\bar{1}2]$ ($\overline{\Gamma} \rightarrow \overline{M}'$) azimuth of the Al(111) SBZ with $\hbar\omega = 9.5$ eV. (b) Dispersion plot of experimentally observed features (labeled as $T1$, $T2$, A'', and B'') and theoretically calculated direct bulk transitions (dashed lines) along the $[\bar{1}\bar{1}2](\overline{\Gamma} \rightarrow \overline{M}')$ azimuth. The hatched area indicates the projected bulk band gap. The shaded area and the crossed solid curve show the dispersions of predicted (Ref. 37) surface resonances.
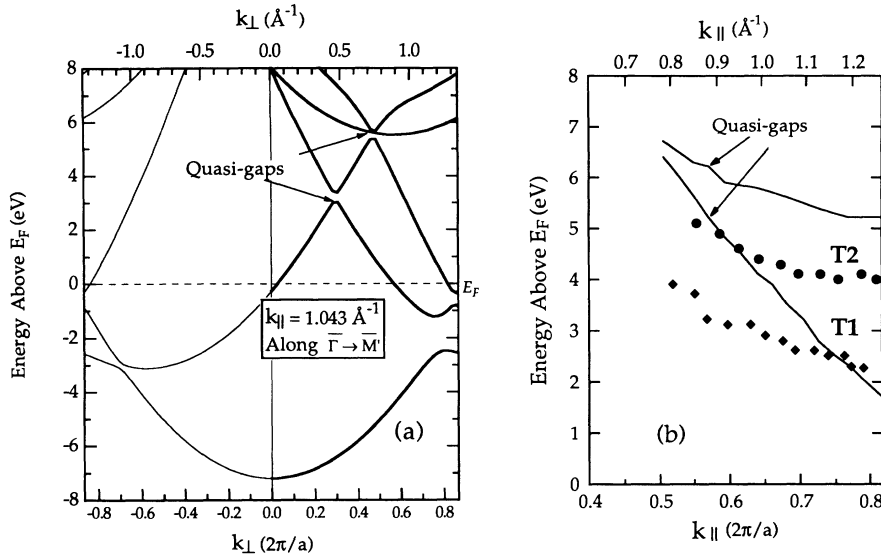
FIG. 6. (a) Results of the self-consistent pseudopotential calculation for the Al(111) bulk electron energy bands as a function of $k_\perp$ at $k_\parallel = 1.043$ Å^{-1} along the $[\bar{1}\,\bar{1}2]$ ($\bar{\Gamma} \rightarrow \bar{M}'$) azimuth of the SBZ. Two quasi-band-gaps are indicated. (b) Comparison of the $E(k_\parallel)$ dispersions along the $\bar{\Gamma} \rightarrow \bar{M}'$ azimuth of the two quasi-band-gaps identified in panel (a) and the KRIPE spectral features $T1$ and $T2$.

tion of Ref. 37. It initially follows the dispersion of $T2$ but then moves away from the data, continuing to lower energy with increasing $k_\parallel$ and finally entering the small band gap at the zone boundary. A closer examination of the spectra in Fig. 5(a) suggests that there may be some structure between $T1$ and $T2$, possibly related to this predicted resonance, but the spectral features are too broad to allow us to make a definitive comment. The upper quasigap in Fig. 6(b) remains above $T2$ throughout its dispersion. The first-principles slab calculations[37] did not extend high enough in energy to reveal another surface resonance.

The results in Fig. 6(a) show that the quasigaps themselves are too small and at the wrong energy to account for $T2$. However, throughout the region of the SBZ where it is observed, $T2$ is split off the minimum by a constant energy of 1.25 eV. The fact that the dispersion of $T2$ is parallel to that of the upper quasigap from $k_\parallel \sim 0.85$ Å^{-1} to the zone boundary at $\bar{M}'$ suggests a possible relationship. Closer examination of Fig. 6(a) shows that there is a relatively flat band passing through the quasigap that does not interact with the surrounding states. Analysis of the SCP calculation shows that this band is odd with respect to the mirror plane perpendicular to a $\langle \bar{1}10 \rangle$ vector (i.e., the plane which contains the surface normal and a $\langle \bar{1}\,\bar{1}2 \rangle$ vector) while all the other states in this region are even. Therefore an energy gap exists below this band minimum [~ 5 eV in Fig. 6(a)] for states of odd symmetry. We propose that $T2$ is an odd surface state in this symmetry gap, following the band minimum as it disperses to lower energy with increasing $k_\parallel$. The band minimum is very close in energy to the upper quasigap, thereby explaining the similarity between its dispersion and that of $T2$ seen in Fig. 6(b).

An additional piece of evidence which supports the identification of $T2$ as a surface state is provided by the work of Pellerin and co-workers.[42,43] They have studied the low-energy excitation of the Al(111) surface by using electron-energy-loss spectroscopy (EELS). Two features were observed in their EELS measurements at energy

losses of 1.5–2 and 4–5 eV. The 4–5eV feature has been found to be surface sensitive. We believe that the 4–5 eV loss feature in EELS (Refs. 42,43) is a transition from the filled states at the Fermi level to the empty surface state $T2$ near the zone boundary.
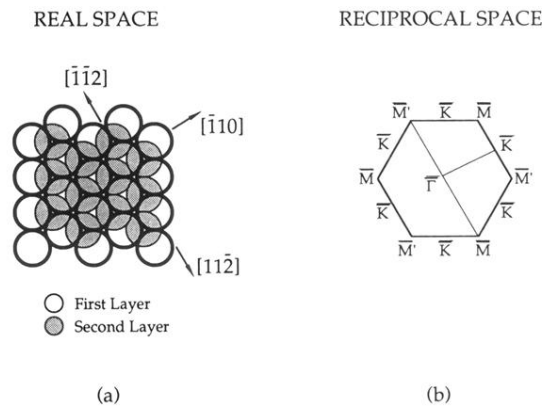
IV. CONCLUSION

We have studied the unoccupied electronic states of Al(111) using k-resolved inverse-photoemission spectroscopy. A first-principles calculation of the bulk electronic structure has also been performed to aid in interpretation of the experimental data. The experimental measurements along the $[\bar{1}10]$, $[11\bar{2}]$, and $[\bar{1}\,\bar{1}2]$ azimuths of the SBZ were characterized by well-defined features within 5 eV of the Fermi level. In addition, broad, weak features occurred at high energies. A weak but well-defined dispersing spectral feature in the $[\bar{1}10]$ direction is identified as a bulk direct transition. A semiquantitative account of its dispersion is obtained by modifying the results of the self-consistent pseudopotential calculation to account for excitation effects.[39] A strong spectral feature found along the $[11\bar{2}]$ azimuth is the unoccupied continuation of a dispersing surface resonance previously observed in angle-resolved photoemission[6] and surface electronic-structure calculations.[34,37] An odd surface state observed along the $[\bar{1}\,\bar{1}2]$ direction occurs in a symmetry gap and is believed to participate in a surface-sensitive transition observed in earlier EELS studies of this surface.[42,43]

ACKNOWLEDGMENTS

*Present address: Department of Physics, University of Texas at Arlington, P.O. Box 19059, Arlington, TX 76019-0059.

[1]J. R. Anderson and S. S. Lane, Phys. Rev. B **2**, 298 (1970).

[2]H. Ehrenreich, H. P. Philipp, and B. Segall, Phys. Rev. **132**, 1918 (1963).

[3]A. G. Mathewson and H. P. Myers, J. Phys. F **2**, 403 (1972).

[4]H. J. Levinson, F. Greuter, and E. W. Plummer, Phys. Rev. B **27**, 727 (1983).

[5]S. D. Kevan, N. G. Stoffel, and N. V. Smith, Phys. Rev. B **31**, 1788 (1985).

[6]G. V. Hansson and S. A. Flodström, Phys. Rev. B **18**, 1562 (1978).

[7]E. Jensen, R. A. Bartynski, T. Gustafsson, E. W. Plummer, M. Y. Chou, M. L. Cohen, and G. B. Hoflund, Phys. Rev. B **30**, 5500 (1984).

[8]E. Jensen and E. W. Plummer, Phys. Rev. Lett. **55**, 1912 (1985).

[9]R. A. Bartynski, R. H. Gaylord, T. Gustafsson, and E. W. Plummer, Phys. Rev. B **33**, 3644 (1986).

[10]I.-W. Lyo and E. W. Plummer, Phys. Rev. Lett **60**, 1558 (1988).

[11]S. P. Singhal and J. Callaway, Phys. Rev. B **16**, 1744 (1977).

[12]N. V. Smith, Rep. Prog. Phys. **51**, 1227 (1988).

[13]V. Dose, Surf. Sci. Rep. **5**, 337 (1985).

[14]F. J. Himpsel, Comments Condens. Matter Phys. **12**, 199 (1986).

[15]D. Heskett, K.-H. Frank, E. E. Koch, and H.-J. Freund, Phys. Rev. B **36**, 1276 (1987).

[16]W. Drube, F. J. Himpsel, and P. J. Feibelman, Phys. Rev. Lett. **60**, 2070 (1988).

[17]P. J. Feibelman, Phys. Rev. Lett. **34**, 1092 (1975).

[18]P. J. Feibelman, Phys. Rev. B **12**, 1319 (1975).

[19]H. J. Levinson, E. W. Plummer, and P. J. Feibelman, Phys. Rev. Lett. **43**, 952 (1979).

[20]S. Yang, R. A. Bartynski, G. P. Kochanski, S. Papadia, T. Fondén, and M. Persson, Phys. Rev. Lett. **70**, 849 (1993).

[21]P. A. Bruhwiler, G. M. Watson, E. W. Plummer, H.-J. Sagner, and K.-H. Frank, Europhys. Lett. **11**, 573 (1990).

[22]R. G. Dandrea and N. W. Ashcroft, Phys. Rev. B **32**, 6936 (1985).

[23]P. M. Echenique and J. B. Pendry, J. Phys. C **11**, 2065 (1978).

[24]N. V. Smith, Phys. Rev. B **32**, 3549 (1985).

[25]B. Frick, K. Jacobi, J. A. Wilder, H. J. Sagner, and K. H. Frank, Surf. Sci. **192**, 529 (1988).

[26]S. Papadia, M. Persson, and L.-A. Salmi, Phys. Rev. B **41**, 10 237 (1990).

[27]M. Radny, Surf. Sci. **231**, 43 (1990).

[28]S. Å. Lindgren and L. Walldén, Phys. Rev. B **40** (1989).

[29]W. L. Schaich and J. T. Lee, Phys. Rev. B **44**, 5973 (1991).

[30]S. Yang, K. Garrison, and R. A. Bartynski, Phys. Rev. B **43**, 2025 (1991).

[31]N. W. Ashcroft, Philos. Mag. **8**, 2055 (1963).

[32]D. R. Hamann, M. Schlüter, and C. Chiang, Phys. Rev. Lett. **43**, 1494 (1979).

[33]D. Vanderbilt, Phys. Rev. B **32**, 8412 (1985).

[34]D.-S. Wang, A. J. Freeman, H. Krakauer, and M. Posternak, Phys. Rev. B **23**, 1685 (1981).

[35]J. R. Chelikowski, M. Schlüter, S. G. Louie, and M. L. Cohen, Solid State Commun. **17**, 1103 (1975).

[36]K. Mednick and L. Kleinman, Phys. Rev. B **22**, 5768 (1980).

[37]M. Heinrichsmeier, A. Fleszar, and A. G. Eguiluz, Surf. Sci. **285**, 129 (1993).

[38]L. Hedin and S. Lundqvist, in *Solid State Physics: Advances in Research and Applications,* edited by F. Seitz, P. Turnbull, and E. Ehrenreich (Holt, Reinhardt and Winston, New York, 1969), p. 1.

[39]J. E. Northrup, M. S. Hybertsen, and S. G. Louie, Phys. Rev. B **39**, 8198 (1989).

[40]E. W. Plummer, Surf. Sci. **152/153**, 162 (1985).

[41]S. G. Louie, P. Thiry, R. Pinchaux, Y. Petroff, D. Chandesris, and J. Lecante, Phys. Rev. Lett. **44**, 549 (1980).

[42]F. Pellerin, J. P. Langeron, M. Gautier, and C. L. Gressus, Phys. Rev. B **30**, 1012 (1984).

[43]M. Gautier, C. L. Gressus, and F. Pellerin, Surf. Sci. **162**, 74 (1985).

REAL SPACE   RECIPROCAL SPACE

$[\bar{1}\bar{1}2]$

$[\bar{1}10]$

$[11\bar{2}]$

○ First Layer
◉ Second Layer

$\overline{M}'$ $\overline{K}$ $\overline{M}$
$\overline{K}$ $\overline{K}$
$\overline{M}$ $\overline{\Gamma}$ $\overline{M}'$
$\overline{K}$ $\overline{K}$
$\overline{M}'$ $\overline{K}$ $\overline{M}$

(a)   (b)

FIG. 1. Geometry of the fcc (111) surface in (a) real space and (b) reciprocal space. Note that the inequivalence of the $[11\bar{2}]$ and $[\bar{1}\,\bar{1}2]$ directions is illustrated by the presence of the second layer in panel (a).
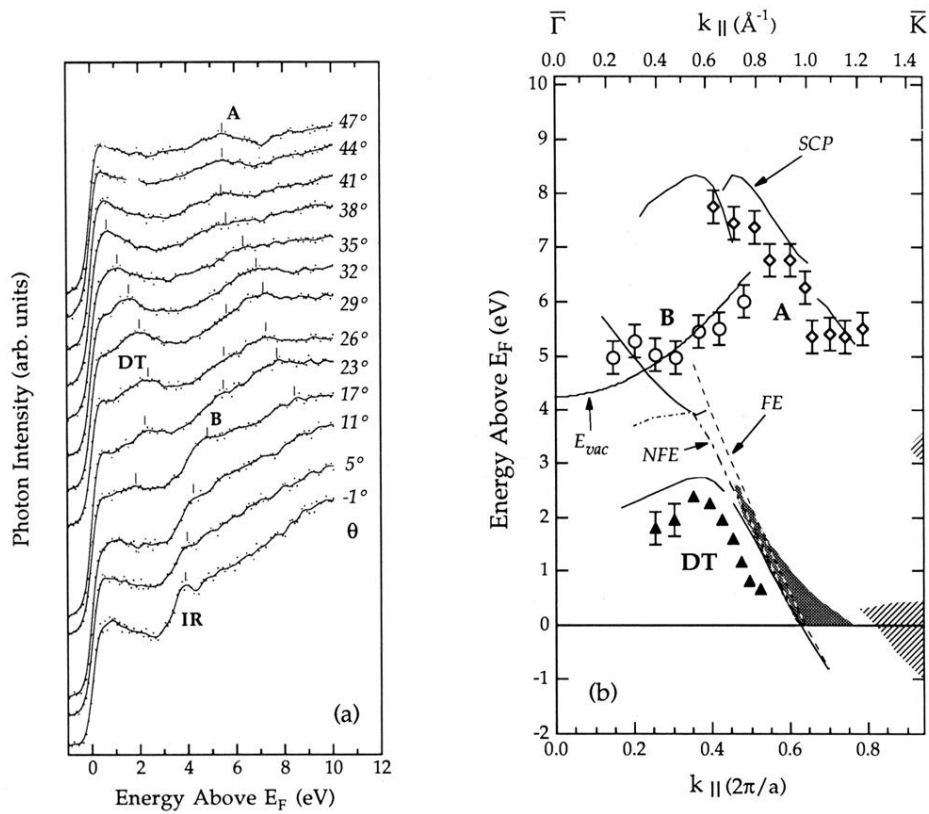
FIG. 2. (a) **KRIPE** isochromat spectra from Al(111) as a function of incident electron angle θ along the $[\bar{1}10]$ ($\bar{\Gamma} \rightarrow \bar{K}$) azimuth of the Al(111) SBZ with $\hbar\omega = 9.5$ eV. (b) Dispersion plot of experimentally observed features (labeled as **DT**, *A*, and *B*) and theoretically calculated direct bulk transitions along the ($\bar{\Gamma} \rightarrow \bar{K}$) azimuth. Results assuming free-electron (**FE**), nearly-free-electron (**NFE**), and the self-consistent l-dependent pseudopotential (**SCP**) bands are given by the dashed, dashed-and-dotted, and solid curves, respectively. Hatched areas indicate the projected bulk band gaps and shaded area shows a predicted surface resonance (Ref. 37).
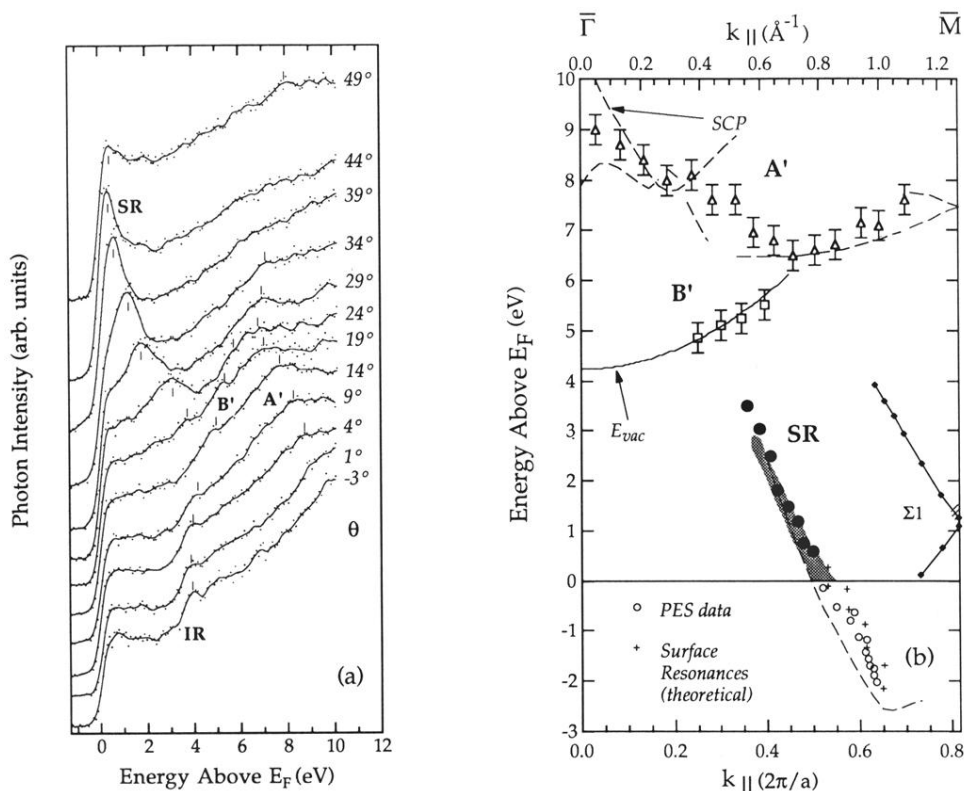
FIG. 3. (a) **KRIPE** isochromat spectra from Al(111) as a function of incident electron angle θ along the $[11\bar{2}]$ ($\bar{\Gamma} \rightarrow \bar{M}$) azimuth of the Al(111) SBZ with $\hbar\omega = 9.5$ eV. (b) Dispersion plot of experimentally observed features (labeled as SR, A', and B') and theoretically calculated direct bulk transitions (dashed lines) along the $[11\bar{2}]$ ($\bar{\Gamma} \rightarrow \bar{M}$) azimuth. Relevant calculated direct transition curves from the SCP bands are shown. Photoemission data (open circles) (Ref. 6) and the calculated (Ref. 32) dispersion of a surface resonance (crosses) are included for comparison. The hatched area indicates the projected bulk band gap and the shaded area shows the predicted (Ref. 37) dispersion of the surface resonance above E_F.
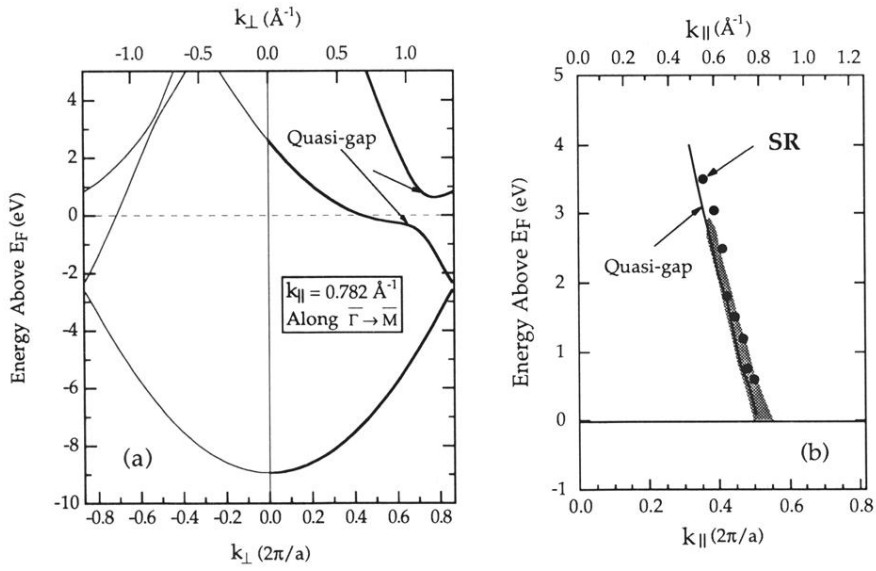
FIG. 4. (a) Self-consistent pseudopotential calculation for Al(111) bulk electron energy bands as a function of $k_\perp$ at $k_\parallel = 0.782$ Å^{-1} along the $[11\bar{2}](\bar{\Gamma} \to \bar{M})$ azimuth of the SBZ. Indicated is the quasi-band-gap. (b) Comparison of the $E(k_\parallel)$ dispersions, along the $[11\bar{2}]$ $(\bar{\Gamma} \to \bar{M})$ azimuth of the Al(111) SBZ, of the quasi-band-gap from panel (a) and the KRIPE spectral feature SR.

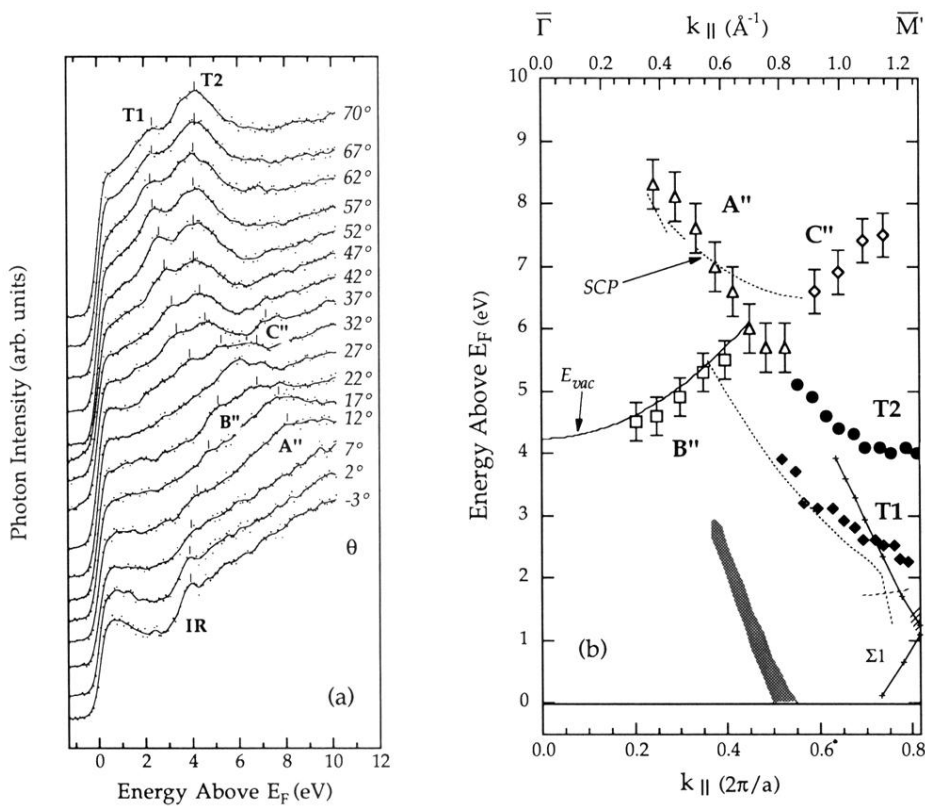FIG. 5. (a) **KRIPE** iso-chromat spectra from Al(111) as a function of incident electron angle θ along $[\bar{1}\,\bar{1}2]$ ($\overline{\Gamma}\rightarrow\overline{M'}$) azimuth of the Al(111) SBZ with $\hbar\omega = 9.5$ eV. (b) Dispersion plot of experimentally observed features (labeled as $T1$, $T2$, A'', and B'') and theoretically calculated direct bulk transitions (dashed lines) along the $[\bar{1}\,\bar{1}2]$($\overline{\Gamma}\rightarrow\overline{M'}$) azimuth. The hatched area indicates the projected bulk band gap. The shaded area and the crossed solid curve show the dispersions of predicted (Ref. 37) surface resonances.